Multiple Planetary Flow Regimes in the Southern Hemisphere

By Shigeo Yoden, Masato Shiotani and Isamu Hirota

Geophysical Institute, Kyoto University, Kyoto 606, Japan
(Manuscript received 1 December 1986, in revised form 5 June 1987)

Abstract

An observational study is made of low-frequency variations of the general circulation in the Southern Hemisphere troposphere with the aid of daily data analyzed at the National Meteorological Center (NMC).

In the winter of 1983 there exist two typical patterns of the zonal mean geostrophic wind in the meridional plane. We name them the single jet regime and the double jet regime, each of which persisted with a characteristic duration of a month and appeared twice alternatively. In the single jet regime, the subtropical jet at the tropopause level is strong and the stationary wave of zonal wavenumber (WN =) 3 has a larger amplitude than WN = 2. On the other hand, in the double jet regime the subtropical jet is weak and the polar night jet extends down to the surface at about 55°S. Dominant stationary planetary waves are WN = 1 and 2. These two regimes are also observed in the three years 1980–1982.

In terms of the quasi-geostrophic Eliassen-Palm (E-P) flux diagnostics, the vertical component of the E-P flux, which is proportional to the horizontal eddy heat flux, is larger around the mid-latitude troposphere in the single jet regime than in the double jet regime. Consequently, the convergence of the E-P flux, which acts as a wave drag on the mean westerly wind, is larger around the mid- and high latitude tropopause level in the single jet regime than in the double jet regime. The larger wave drag tends to keep the weaker westerlies in the single jet regime.

An empirical orthogonal function (EOF) analysis is made to define an index of the zonal mean wind of two dimension. The first component of EOF, which represents over 40% of the total variance, corresponds to the variations between the two regimes. The amplitude of this component is used as a kind of 'zonal index'. Time-variation of the zonal index is not considered an internal oscillation with an intrinsic frequency because the 'period', which is not an appropriate concept for the present phenomenon, is different in each year. The transition between the regimes is rather rapid compared with the duration of each regime. No clear relation is found between the regime transitions and the annual variation. These observational evidences support an interpretation that this low-frequency variation of the zonal index is the transition between multiple planetary flow regimes in the Southern Hemisphere.

1. Introduction

It is well known that the general circulation of the atmosphere has low-frequency variability with time scales of a week or longer. Wallace and Blackmon (1983) documented some of the characteristics of the low-frequency variations by reviewing recent observational studies and also discussed some causes of them by referring theoretical works. However, as mentioned by themselves there still exists an enigma of the low-frequency atmospheric variability.

In this paper we show another observational example of low-frequency variations in the Southern Hemisphere troposphere. It is an irregular fluctuation of zonal mean geostrophic winds during wintertime. The fluctuation is characterized by the persistence with characteristic duration of a month and rather rapid transition to another state.

One possible interpretation of this low-frequency variation is the transition between

©1987, Meteorological Society of Japan

different climatic regimes, which is one of the six causes exemplified by Wallace and Blackmon (1983). They stated that there is a possibility of two or more preferred climatic states that might coexist in the presence of the same external forcing. The multiplicity of climatic regimes may be permitted to exist because the atmosphere is a highly nonlinear system. Theoretical background of this concept was introduced by Lorenz (1968) in terms of the 'almost-intransitive system' and revived by Charney and DeVore (1979) in the problem of blocking.

There are some observational studies on the multiplicity of climatic states. Dole (1982) investigated the persistent anomalies of wintertime circulation well known as blocking phenomena. He showed that the duration of individual anomaly events is highly variable and that the development and decay of these events are rather abrupt compared with the duration. Wallace and Blackmon (1983) gave a similar example of two different flow regimes over the Rocky mountains. One regime is related to the Pacific/North American correlation pattern (Wallace and Gutzler, 1981) and the other is very similar to the long-term climatology. They used a subjective approach to identify the circulation patterns associated with preferred flow regimes, but it is justifiable in the absence of detailed theoretical guidance. In these studies climatic states were defined regionally.

On the other hand, there are some observational studies in which the climatic state is defined in the hemisphere. Sutera (1986) made an analysis of the 500 mb geopotential height field in the Northern Hemisphere winter. He found that a measure of the planetary wave components of the atmospheric flow has a bimodal density distribution, *i.e.*, two preferred kinetic energy levels. Mo and Ghil (1987) obtained two types of persistent 500 mb height anomalies with distinct statistical features in the Southern Hemisphere. They tried to explain these anomalies as belonging to multiple planetary flow regimes by making the same analysis for an idealized dynamical model by Legras and Ghil (1985).

Our approach is different from those in the previous studies cited above; we mainly take note of the day-to-day variation of the zonal mean wind as an index of the variation of planetary-scale (hemispheric) flow. Time-variations of zonally asymmetric components are also investigated in relation to those of the zonal mean. The reason why we choose the Southern Hemisphere is that the contamination of the forced annual variation is small compared with the Northern Hemisphere. (In this study we are interested in the transition between different climatic regimes, which is essentially free variation of the atmosphere.) The smallness of the annual variation is explained by the fact that a large part of the Southern Hemisphere is covered by the ocean, which has a large heat capacity.

We use the NMC data for four years from 1980 to 1983. Description of the data set is given in Section 2. Variations of the general circulation in 1983 are investigated first in detail: Variations of the zonal mean geostrophic wind are described in Section 3 and those of zonally asymmetric components in Section 4. In Section 5 a similar investigation is made for the other three years in order to reveal the characteristic variations more clearly. Relations to previous observational studies and numerical model works are discussed in Section 6 and the conclusions are given in Section 7.

2. The data set

Our data are the NMC daily geopotential height and temperature analyses in the Southern Hemisphere for 12 pressure levels from 1000 mb up to 50 mb. For a detailed description of the data sources and analysis procedure, see Geller *et al.* (1983). Originally the NMC analyses covered the globe with 2.5° × 2.5° longitude-latitude grids at twice-daily intervals. In order to reduce the data we adopted a coarse grid of 5° × 5° in the Southern Hemisphere and used only once daily analysis at 1200 GMT.

The analyzed period is four years from January 1980 to December 1983. There exist five periods in which the data are continuously missing for seven days or more: February 1 – 7, 1981; August 30 – September 5, 1981; October 4 – 10, 1981; June 30 – July 17, 1982 and April 9 – 30, 1983. There also exist sporadically missing data besides these periods but the rate of missing data is 7%. We made a linear interpolation in time for the missing data.

3. Variations of the zonal mean wind in 1983

The zonally averaged geostrophic zonal wind $[u](\varphi, p, t)$ was computed between 5°S and 85°S using a centered difference at intervals of 10° latitude. The notation is listed in Appendix A. Fig. 1 shows time latitude sections of $[u](\varphi, p_1, t)$ at p_1 = 200 mb and 500 mb. The annual variation of $[u]$ is not as large as that in the Northern Hemisphere. In particular the seasonal march in wintertime is not conspicuous from May to October. This feature is more evident at the lower level (500 mb).

In wintertime low-frequency variations with characteristic duration of about a month are dominant. At the 200 mb level, in addition to the primary jet of $[u]$ between 25°S and 35°S, a second maximum in $[u]$ exists at about 50°S from July to August and after September. The position of the westerly jet at 500 mb varies between 30°S and 60°S in concert with the appearance of the secondary jet at 200 mb.

The winter period from June 11 to October 20 (132 days), with which we are mainly concerned, is divided into four periods according to the position of westerly jet (Fig. 1). The subdivided periods are not the same length but all are between 25 days and 41 days (see bottom-left in Fig. 2). Although this division is a subjective one, there are only a few alternatives because of fast transitions of the westerly jet.

The time average and the standard deviation of $[u]$ are computed within each sub-periods (denoted by Period = 1 ~ 4 in the figures) as well as the whole period (Total). Fig. 2 shows the time average $[\bar{u}]$ and $[\bar{u}]$ ± standard deviation of $[u]$ at the 200 mb level for each averaging period. The zonal wind has a single jet profile with a maximum near 30°S for periods 1 and 3. On the other hand, for periods 2 and 4 there exists a secondary maximum of $[\bar{u}]$ at 55°S. The primary jet in the subtropics in these periods is weaker than that in periods 1 and 3. The average for the whole period resembles none of the sub-periods. The resemblance of the $[\bar{u}]$ profile is notable between periods 1 and 3.

The standard deviation of $[u]$ for the whole period takes on large values near 30°S, 60°S and 80°S. At these latitudes variations of $[\bar{u}]$ among sub-periods are large and contribute to the large

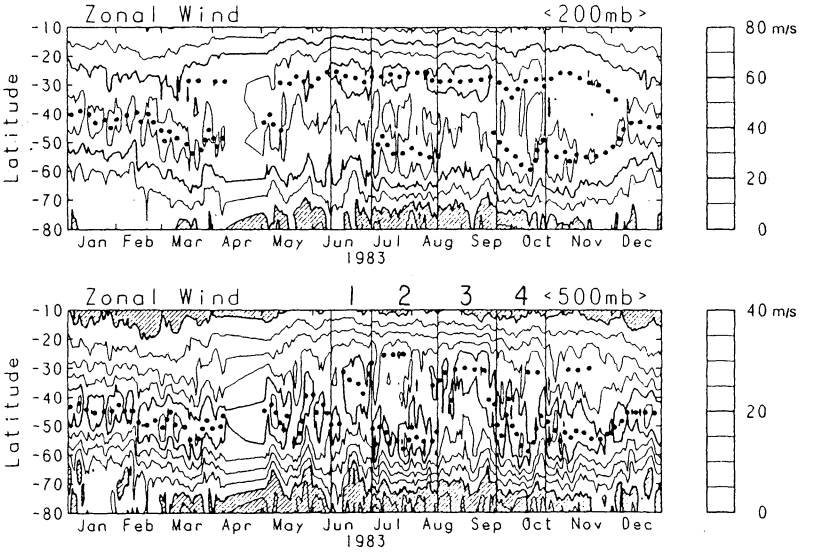

Fig. 1 Time-latitude sections of the zonal-mean geostrophic wind $[u]$ at 200 mb (top) and 500 mb (bottom). Local maximum of $[u]$ (*i.e.*, position of westerly jet) is denoted by dot. Data from April 9 to April 30 are linearly interpolated. Oblique lines are drawn for negative $[u]$ of easterly wind. Winter period is divided into four sub-periods (1 ~ 4), which are bordered by vertical lines.

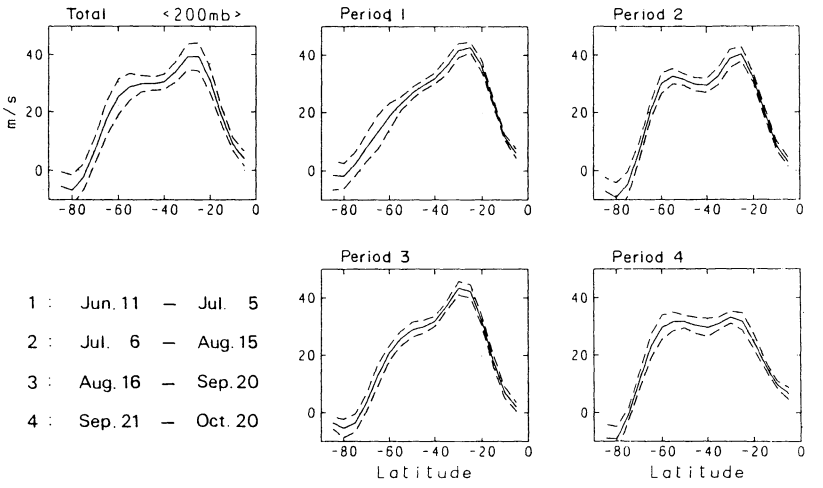

Fig. 2 Meridional profiles of the zonal-mean geostrophic wind at 200 mb averaged in the whole period and in the four sub-periods. Broken lines denote the average ± one standard deviation.

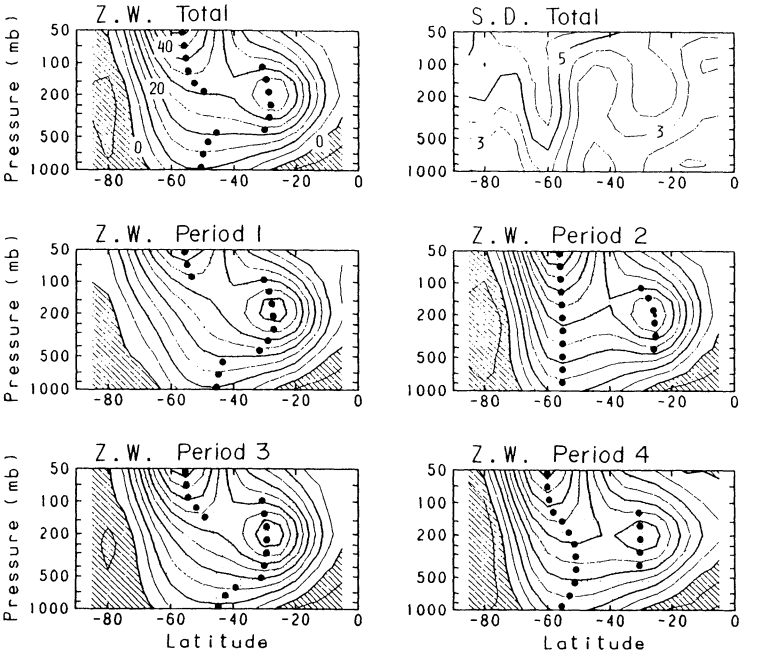

Fig. 3 Meridional cross section of the zonal-mean geostrophic wind averaged in the whole period (top-left) and the sub-periods (middle and bottom). Standard deviation in the whole period is also shown (top-right). Contour interval is 5 ms^{-1} for averaged wind and 1 ms^{-1} for standard deviation.

standard deviation for the whole period. In particular at 60°S the difference of $[\bar{u}]$ between periods 1 and 2 (or 3 and 4) exceeds 10 ms^{-1}. The standard deviation for each sub-period is small at all latitudes except for the polar region.

Meridional cross sections of $[\bar{u}](\varphi, p)$ are shown in Fig. 3 for each averaging period. The top two panels are the average and the standard deviation of $[u]$ for the whole period. The sub-tropical jet has a maximum value of about

40 ms^{-1} at 30°S and 200 mb. The distribution of $[\bar{u}](\varphi, p)$ for the whole period is close to the climatological one for July obtained by Trenberth (1984). The standard deviation for the whole period is largest around 60°S at all levels. There also exists a second maximum near the subtropical jet.

In periods 1 and 3, the subtropical jet is strong and there is no secondary jet at all levels in the troposphere. On the other hand, in periods 2 and 4, the subtropical jet is weak and the polar night jet extends down to the surface at about 55°S, so that a double jet structure is prominent in the upper troposphere. The two-dimensional profiles of $[\bar{u}](\varphi, p)$ in the troposphere resemble one another for periods 1 and 3 and for periods 2 and 4. From now on, we call periods 1 and 3 single jet regime and periods 2 and 4 double jet regime.

In order to see the day-to-day variation of zonal mean winds, an empirical orthogonal function (EOF) analysis in the meridional plane is performed on the basis of the cross-covariance matrix of $[u]$. Details of the EOF analysis were reviewed by North *et al.* (1982). It is a good method to obtain a characteristic spatial pattern of the variations, which is given by an eigenvector $E_n(\varphi_i, p_j)$ of the matrix, and to know time-variations of each component by computing an amplitude $A_n(t)$.

We define the amplitude $A_n(t)$ as

$$A_n(t)=\alpha\times\sum_{i=1}^{17}\sum_{j=1}^{10}E_n(\varphi_i, p_j)\times[u](\varphi_i, p_j, t). \tag{3.1}$$

where φ_i denotes i-th latitude grid and p_j j-th pressure level. Coefficient α is a positive definite to set $A_1 \sim O(1)$. The amplitudes, especially the first component can be used as a kind of 'zonal index'.

EOF patterns $E_n(\varphi, p)$ for the largest two components are shown in Fig. 4. Here the data at 50 mb and 70 mb have been discarded because the variations in the stratosphere have a large component of the seasonal march (see, *e.g.*, Shiotani and Hirota, 1985). The variance associated with the first EOF component represents about a half of the total variance of $[u]$ below 100 mb. The eigenvalue is 3.4 times as large as the second one. It is expected the sampling error is small, because this is a case of 'stand out' EOF named by North *et al.* (1982).

There exist two regions with large modulus of E_1: All levels at about 60°S and the upper troposphere at about 25°S. These regions have opposing signs; the variations of this component are out of phase between middle and low latitudes. The sign of E_1 in very high latitudes is the same as that in low latitudes.

Time variations of $A_n(t)$ are presented in Fig. 5. The amplitude $A_1(t)$ has a same sign within the duration of about a month. This component is closely related to the single/double jet regimes; the single jet regime corresponds to negative A_1 (= $-1.5 \sim -2$) and the double jet regime to positive A_1 (= $1 \sim 2$). High-frequency variations are seen around the average values over each period (the dotted lines in Fig. 5). In the time-variations of A_1, the transitions from one regime to the other are very rapid compared with the duration of each regime. This feature reminds us of typical variations in an almost intransitive system. A possibility of the oscillation with an intrinsic period of about two months will be denied in Section 5.

The second component EOF2 has a connection with variations in the stratosphere. At the highest levels $E_2(\varphi, p)$ has opposing maxima in

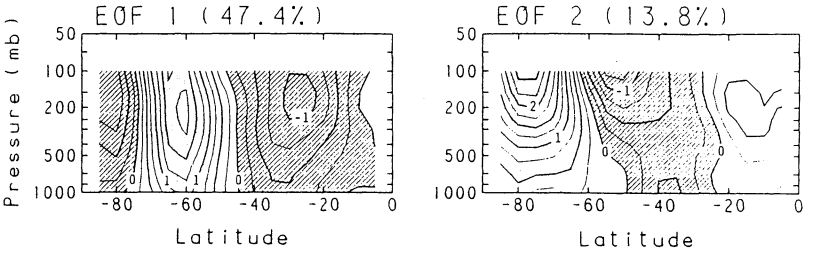

Fig. 4 EOF patterns E_n of the zonal-mean geostrophic wind (n = 1 and 2). Negative values are over oblique lines.

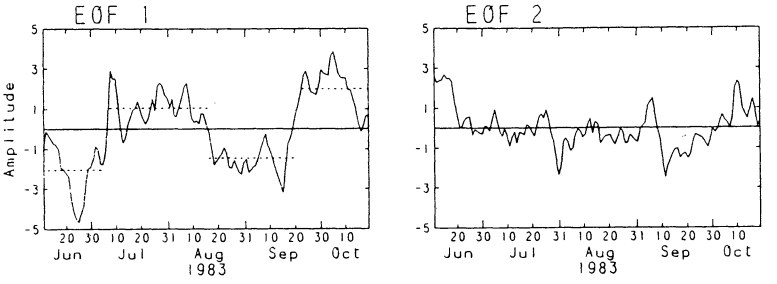

Fig. 5 Time variation of EOF amplitude A_n. In the panel of EOF 1 the average value in each sub-period is drawn by a dotted line.

middle and high latitudes. The amplitude A_2 has a seasonal variation with largest negative values during winter. Some intermittent variations with time-scales of a few weeks are superposed on the seasonal march. Large changes occur at the end of July and at the beginning of September. In both periods an abrupt decrease follows a more gradual buildup of A_2. Time-variations of A_2 bear a close relation to the seasonal variation in the Southern Hemisphere stratosphere (Shiotani and Hirota, 1985).

4. Variations of zonally asymmetric components in 1983

Non-zonal components such as planetary waves, long waves and local disturbances appear to have some variations related to the single/double jet regimes. Fig. 6 shows the geopotential height at the 500 mb level averaged over the whole period (Total) and the sub-periods 1 ~ 4. The shaded area is where the zonal component of the geostrophic wind $\bar{u}$ exceeds 20 ms^{-1}. Average values over the whole period can be compared with similar climatic charts by Trenberth (1979, 1982). The resemblance is well at first sight. There exists a difference in the Pacific Ocean (90°W–150°W); the zonal component of geostrophic winds for this year is smaller than that obtained over a long period by Trenberth (1982), although the difference might be related with the difference between the data sets.

If we take an average over each sub-period, however, the geopotential height fields are different from that for the whole period. Meanders of the isopleths are conspicuous in periods 1 and 3. A wavenumber three pattern in middle latitudes is striking for period 3.

Fig. 7 shows a result of Fourier harmonic

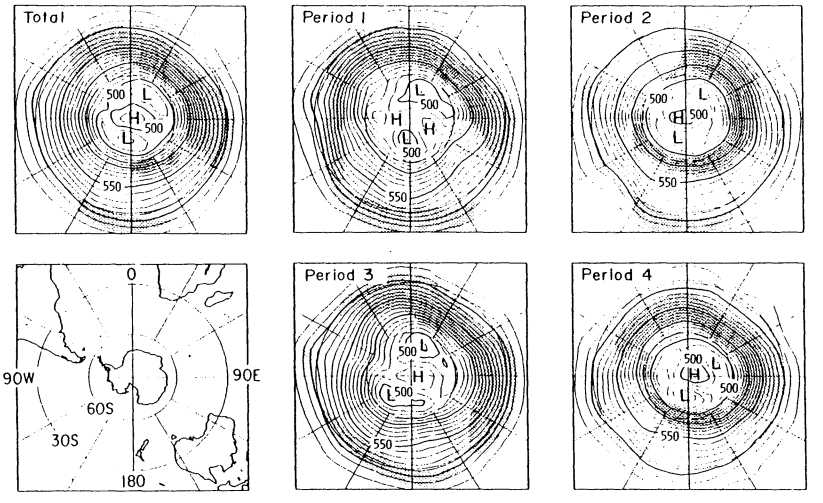

Fig. 6 Geopotential height (unit: dam) at 500 mb averaged in the whole period and four sub-periods. Shaded area is where the zonal component of geostrophic wind exceeds 20 ms^{-1}.

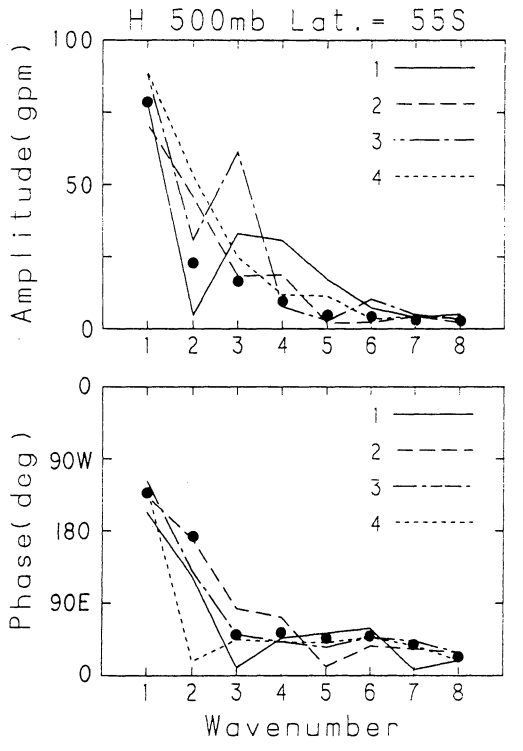

Fig. 7 Amplitude and phase of the stationary height wave along 55°S in Fig. 6. Average in the whole period is denoted by dot and those in the sub-period by four different lines.

analysis along 55°S. The amplitude and phase of the stationary waves in the geopotential height were computed for the whole period and the sub-periods. The phase is defined as a position of maximum in longitude. It is apparent that amplitudes and their variations among sub-periods are large for planetary waves (WN = 1 ~ 4). The amplitude and phase of WN = 1 do not vary significantly among sub-periods (about 80 gpm and 130°W). The difference mainly comes from WN = 2 ~ 4. In period 1 both WN = 3 and 4 have larger amplitudes (30 gpm) than WN = 2 and in period 3 WN = 3 attains 60 gpm of amplitude. In periods 2 and 4, on the other hand, WN = 2 has a larger amplitude than WN = 3 and 4. Thus, in the single jet regime the stationary planetary wave of WN = 3 (or 3 and 4) is prominent while WN = 2 is in the double jet regime. The predominance of WN = 3 (and 4) in periods 1 and 3 has a close relation to some diffluent flow patterns in middle latitudes (Fig. 6): 120°E–150°E in period 1; 150°E–180° and 60°W–90°W in period 3. This kind of flow pattern is suggestive of persistent blocking events.

Areas of strong zonal winds also vary among the sub-periods. The variation is large in the Pacific Ocean (150°E–90°W); strong zonal winds blow along 30°S in periods 1 and 3, and along 60°S in periods 2 and 4. In the south Indian Ocean, on the other hand, strong zonal winds of over 25 ms^{-1} blow along 45°S but the difference among the sub-periods is not noticeable. The variation in the Pacific Ocean is related to that of the zonal mean wind described in the previous section.

The intensification of the zonal wind around 60°S in periods 2 and 4 has some relation to the deepening of the polar vortex. If we pay attention to a particular isopleth, say, 500 dam, it is along 60°S in these periods. On the other hand, there is no circumpolar isopleth of 500 dam in periods 1 and 3.

To see the nature of time-variations of the zonally asymmetric component we show the Hovmöller diagrams. Figs. 8 and 9 are time-longitude sections of the height wave (defined as deviation from the zonal mean in each day) along two latitudinal bands, 40°S–50°S and 20°S–30°S, respectively. In the figures a running-mean of 5 days and Fourier composition of WN = 1 ~ 8 were taken to remove the high-frequency and small-scale components.

In middle latitudes (Fig. 8) the disturbances have large amplitudes in periods 1 and 3. In periods 2 and 4, on the contrary, there are a few disturbances with large amplitudes. This feature is not clear in lower latitudes (Fig. 9). Namely, there appear large amplitude disturbances in some periods but they have little relation to the single/double jet regimes.

If we take note of individual disturbances, we can observe rather persistent highs with a large amplitude in middle latitudes accompanied by low-pressures in low latitudes (marked by A–D in Figs. 8 and 9). The phase speed is small compared with other disturbances. The longitudes of these highs correspond to those of the diffluent flow patterns in Fig. 6. These disturbances might be identified as persistent blocking highs.

In these time-longitude sections, we sometimes observe wavetrains with intensified troughs and ridges (*e.g.*, X and Y in Figs. 8 and 9). These

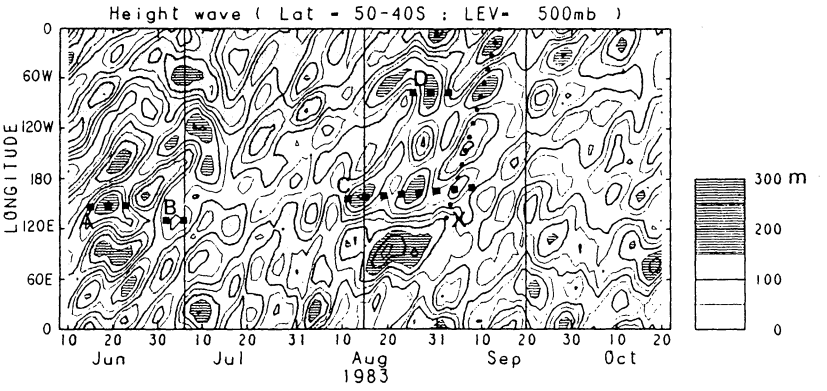

Fig. 8 Time-longitude section of height wave (deviation from the zonal mean in each day) at 500 mb. Average over three latitudes between 50°S and 40°S is shown. Contour interval is 50 m and negative value is shaded by dots. Vertical lines divide the whole period into four sub-periods.

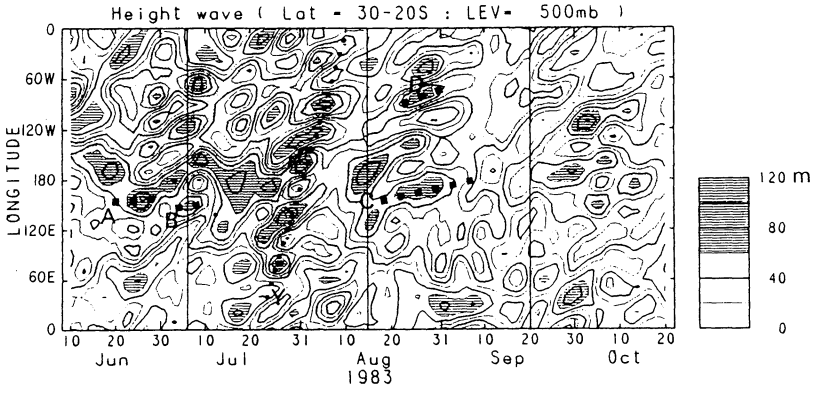

Fig. 9 As in Fig. 8 but for the latitudes between 30°S and 20°S. Contour interval is 20 m.

do not seem to have any relation to the single/double jet regimes, but it is interesting to note that these wavetrains roughly satisfy a relation $c + c_g = 2\,[u]$ derived from the dispersion relation of one dimensional Rossby waves (c: phase velocity and c_g: group velocity). The gradient of dotted lines X and Y in the figures gives the group velocity c_g.

Next we describe differences in wave activity between the single and double jet regimes, by presenting the quasi-geostrophic E–P flux and its divergence. In details about the formalism of the E–P flux diagnostics, the reader may consult with Edmon *et al.* (1980) and Dunkerton *et al.* (1981). We briefly write down the definition of the quasi-geostrophic E–P flux **F** and wave driving D_F as

$$\mathbf{F}=(F(\varphi),\ F(z)), \tag{4.1}$$

where

$$F(\varphi)=-\rho a\cos\varphi[u^*v^*] \tag{4.2}$$

$$F(z)=+\rho a\cos\varphi\left(\frac{f}{N^2}\right)[v^*\Phi_z^*], \tag{4.3}$$

and

$$D_F=\frac{1}{\rho a\cos\varphi}\nabla\cdot\mathbf{F} \tag{4.4}$$

where

$$\nabla\cdot\mathbf{F}=\frac{1}{a\cos\varphi}\frac{\partial(F(\varphi)\cos\varphi)}{\partial\varphi}+\frac{\partial F(z)}{\partial z}. \tag{4.5}$$

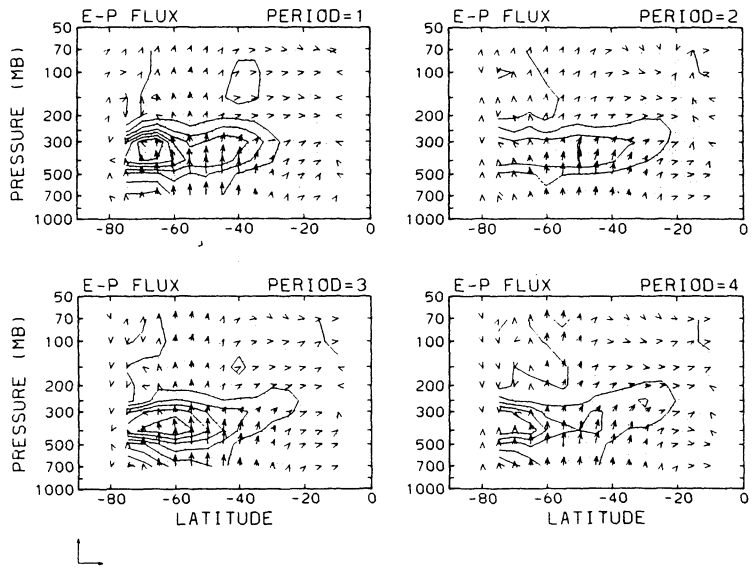

Fig. 10 Latitude-height sections of the E–P flux $\mathbf{F}$ and wave driving $\overline{D_F}$ for the four periods. Contour interval of $\overline{D_F}$ is 2.5×10^{-5} ms^{-2}; negative values are shaded. Reference arrow shows 1.0×10^9 kgs^{-2} for horizontal direction and $1.0 \times 10^9/c$ (c = 317) kgs^{-2} for vertical direction. (See text for the scaling).

The wind field was estimated geostrophically from the geopotential height data and wave component was used from WN = 1 ~ 6. The result is essentially similar even if we take into account of higher wavenumber components. Hereafter we refer to $F(\varphi)$ as $F(y)$.

To extract the difference of wave behavior among the four periods we show period-mean latitude-height cross sections of the E–P vectors $\mathbf{F}$ and wave driving $\overline{D_F}$ (Fig. 10). They were calculated from averages of daily values, not from the period mean field. In plotting the E–P flux in the meridional cross-section we follow the graphical convention as described by Baldwin *et al.* (1985); we have multiplied $\mathbf{F}$ by the factor exp (z/H).

From Fig. 10 we see that:

(1) General pattern of E–P vectors for each of the four periods resembles climatological observations such as Karoly (1982) and Mechoso *et al.* (1985); the E–P vectors point upward from the troposphere to the stratosphere, turn equatorward in the mid-latitude upper troposphere, and point almost equatorward at low latitudes.

(2) Maximum $\overline{F(z)}$ around 50°S in the troposphere is larger in periods 1 and 3 than in periods 2 and 4; values of $\overline{F(z)}$ at 50°S and 500 mb for the four periods are 1.16, 0.88, 1.12 and 0.75 ($\times 10^6$ kg s^{-2}), respectively. On the other hand, $\overline{F(z)}$ in the stratosphere is larger in periods 3 and 4 than in periods 1 and 2. This is consistent with the observational result by Shiotani and Hirota (1985); they showed that the stratospheric wave activity during the 1981 winter in the Southern Hemisphere was more vigorous in late winter than in early winter.

(3) The difference of $\overline{F(y)}$ among the four periods is not as clear as that of $\overline{F(z)}$ from these figures. However, it has larger positive values (equatorward) at mid-latitudes in periods 2 and 4 than in periods 1 and 3; values of $\overline{F(y)}$ at 35°S and 300 mb for the four periods are 5.05, 6.76, 5.70 and 7.67 ($\times 10^7$ kg s^{-2}), respectively. On the contrary, it has larger negative values (poleward) at high latitudes in periods 1 and 3 than in periods 2 and 4; values of $\overline{F(y)}$ at 65°S and 300 mb for the four periods are −2.98, −0.94, −1.41 and −0.43 ($\times 10^7$ kg s^{-2}), respectively.

(4) There is a strong convergence zone of the E–P flux around the 300 – 400 mb at high and mid-latitudes. The wave driving $\overline{D_F}$ has larger negative values in periods 1 and 3 than in periods 2 and 4. This stronger $\overline{D_F}$ in periods 1 and 3 tends to maintain the weaker westerlies around 50–60°S in the troposphere, namely the single jet wind profile. The main contribution of the wave driving $\overline{D_F}$, comes from the vertical derivative of $\overline{F(z)}$.

Wave statistics can be divided into stationary and transient parts. We define the stationary wave as the period-mean height and temperature fields. Then the E–P flux due to the stationary wave is given by

$$\mathbf{F}_s=(F_s(\varphi),\ F_s(z)) \tag{4.6}$$

where

$$F_s(\varphi)=-\rho a\cos\varphi[\bar{u}^*\bar{v}^*] \tag{4.7}$$

$$F_s(z)=+\rho a\cos\varphi\left(\frac{f}{N^2}\right)[\bar{v}^*\bar{\Phi}_z^*]. \tag{4.8}$$

The E–P flux due to the transient wave ($\mathbf{F}_t$) is defined by subtracting $\mathbf{F}_s$ from the total E–P flux, $\overline{\mathbf{F}}$:

$$\mathbf{F}_t=\overline{\mathbf{F}}-\mathbf{F}_s. \tag{4.9}$$

As we showed in Fig. 10 the main difference in wave properties between the single and double jet regimes is characterized by the difference of $\overline{F(z)}$ and consequently wave driving $\overline{D_F}$. Thus we show in Fig. 11 the contribution of stationary and transient waves to the total $\overline{F(z)}$ at 55°S and 400 mb. The latitude and height were selected because the wave driving $\overline{D_F}$ has the largest negative values around this level and $\overline{F(z)}$ has the largest positive values around this latitude.

The contribution of the transient waves is prominent and nearly equal during each period, although there exists a small difference between the two regimes. The difference of the total $\overline{F(z)}$ between the single and double jet regimes is largely contributed by the stationary waves. There is a similar result in Wallace and Blackmon (1983). By using an eddy index E, defined as eddy variance of 500 mb height integrated over the Northern Hemisphere, they contrasted the circulation during high and low index regimes and showed that the higher values of E in the low index regime is mainly due to the larger contribution of the stationary waves.

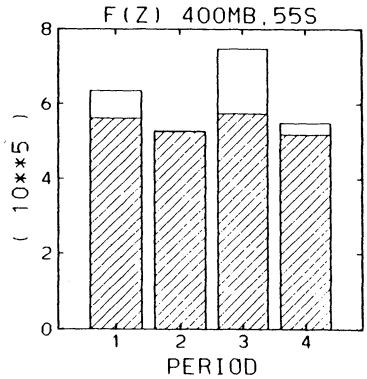

Fig. 11 Bar graph showing contributions of the transient waves (hatched column) and stationary waves (white column) to the total (wavenumber 1 to 6) $\overline{F(z)}$ at 400 mb and 55°S for the four period. Units are 10^5 kgs^{-2}.

5. Variations during 1980–1983

In the previous two sections we described variations in the general circulation during the winter of 1983 in terms of multiple planetary flow regimes, *i.e.*, the single jet regime and the double jet regime. In this section we expand our analysis of zonally averaged geostrophic winds $[u]$ over the four year period 1980–1983 in order to confirm the above discussion.

Figs. 12 and 13 show time-latitude sections of the zonal mean geostrophic wind at the 200 mb and 500 mb levels, respectively. Here we used a low-pass filter (> 30 days) to isolate the low-frequency variations which we are interested in. The adequacy of the filtering is revealed by comparison with the non-filtered result of 1983 in Fig. 1.

Even in the wintertimes of 1980–1982, we can discern single jet regimes and double jet regimes at the 200 mb level, both of which persist for a month or so. A primary jet exists at about 30°S for the winter as a whole. A secondary jet appears at about 50°S–60°S when the primary jet is weak. At the 500 mb level the position of the jet varies between 30°S

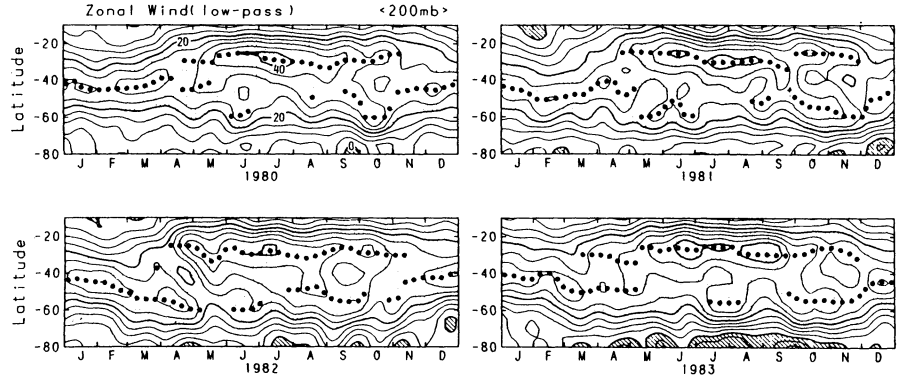

Fig. 12 Time-latitude sections of the zonal mean geostrophic wind (low-pass filtered) at 200 mb. Contour interval is 5 ms^{-1} and easterly wind is over oblique lines. Position of westerly jet is indicated by dot.

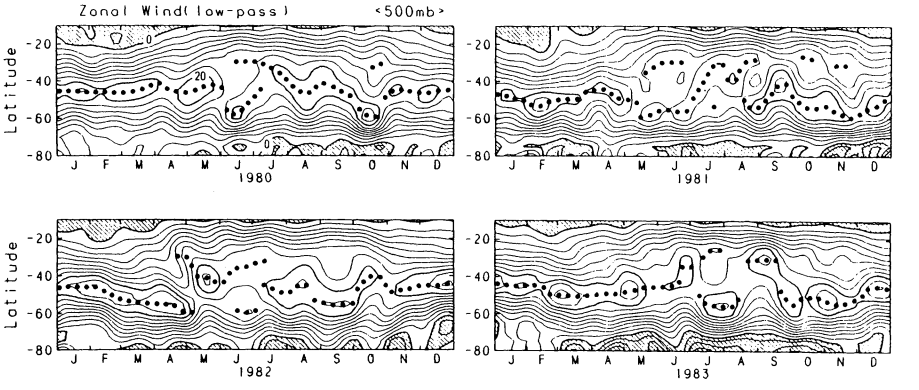

Fig. 13 As in Fig. 12 but for 500 mb level. Contour interval is 2.5 ms^{-1}.

and 60°S. When the double jet appears at the 200 mb level, the primary jet at the 500 mb level is located around 50°S–60°S. In the three years typical episodes characterized by a single jet regime are July 1980 and July–August 1981. On the other hand, typical episodes characterized by double jet regimes are June and October 1980, October–November 1981 and September 1982. Because the appearance of single jet or double jet regimes is not regular, it is difficult to consider the variations to be a result of oscillation or a regular seasonal variation.

The interannual variability is large in the polar region, especially at the 200 mb level. Easterly winds are strong in 1983 compared with the other three years. In low and middle latitudes, where the position of the jet varies in wintertime, variations of the zonal wind $[u]$ from year to year are rather weak.

Again we perform an EOF analysis for four years in order to identify the day-to-day variation about the single/double jet regimes. A cross-covariance matrix is computed from the unfiltered $[u](\varphi, p, t)$ over 528 days from June 11 to October 20 in 1980–1983. Since the interannual variation is prominent in the polar region, we discard the data south of 75°S.

The first EOF pattern E_1 is presented in

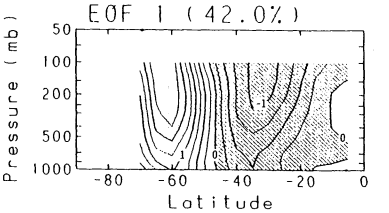

Fig. 14 EOF1 pattern of the zonal-mean geostrophic wind for 528 days (from June 11 to October 20 in 1980–1983).

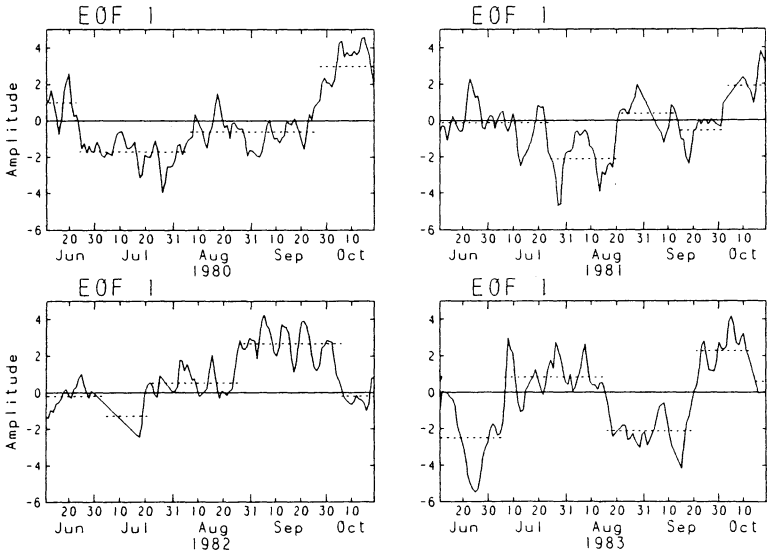

Fig. 15 Time-variation of amplitude A_1 for E_1 defined in Fig. 14. Dotted lines denote averages in each sub-period.

Fig. 14. Compared with Fig. 4, there is little difference of the pattern. The contribution of this component is 42.0% to the total variance and the second component is 17.6%. This is also the case of 'stand out' EOF as in 1983. Therefore the sampling error is expected to be small. The similarity of the spatial pattern $E_1(\varphi, p)$ and the large eigenvalue reveal that the first component obtained in 1983 is also prominent in winter-times 1980–1983.

The amplitude variation is shown in Fig. 15. The dotted lines denote averages of $A_1(t)$ over periods defined subjectively. The variation in 1983 is not much different from that in Fig. 5, because $E_1(\varphi, p)$ has a large modulus in middle and low latitudes. As in 1983 the variation of $A_1(t)$ has a close relation to the single/double jet regimes observed in the other three years. Large positive values of A_1 correspond to the double jet regime and negative ones to the single jet regime. However, there also exist some durations of small A_1 in 1980–1982. These periods of small A_1 might be considered as a third regime.

It is clear that the variations between the regimes do not result from an internal oscillation with an intrinsic frequency, because there is no prominent oscillation with period of about two months in the other three years. Contamination by the seasonal march (the annual variation) does not appear to be a serious problem for the first EOF component. Hence, the low-frequency variation of the zonal index A_1, which is a measure of the variation between the single/double jet regimes, might be considered as an almost intransitive variation with multiple planetary flow regimes. High-frequency fluctuations with periods of about ten days around a mean value and rapid transitions between the regimes support the almost intransitivity.

6. Discussion

Since the appearance of the single/double jet regimes is fundamentally irregular, climatic values of the zonally averaged zonal wind are different depending upon the averaging period. Some of them resemble the single jet regime and some others the double jet regime. In earlier studies there are some examples of the single jet regime: July 1973 (Hartmann, 1977) and July 1972–1977 (Trenberth, 1979, 1984). On the other hand, those of the double jet regime are July 1957–1966 (van Loon, 1972) and July 1979 (Bengtsson *et al.*, 1982).

There have been some discussions suggesting that the difference of climatic values can be understood by the interannual variability or long-term changes (*e.g.*, Trenberth, 1979, 1984). However, we have to be careful when we discuss

the interannual variability by using monthly averaged data, because the variability of zonal mean wind in wintertime is attributed primarily to the alternating appearance of the single and double jet regimes with a characteristic duration of a month. The 'interannual variability' may result from different appearance of the single and/or double jet regimes in a particular month of each year.

Webster and Keller (1975) is the first to investigate the periodic variations of zonal indices, *i.e.*, the vacillations in the Southern Hemisphere. They analyzed the EOLE constant density balloon data set from September 1971 to June 1972 and found that the zonal indices have strong 18–23 day variations. Their cross-spectral analysis suggests that the vacillation appears as a barotropic interaction between the zonal wind and planetary waves. It is interesting to make a comparison between the vacillations and the low-frequency variations obtained here.

The variations between the single and the double jet regimes seem to have little relation to the vacillations. The period, which is not an appropriate concept for the present phenomenon, is about two months in 1983 and much longer in 1980–1982 (Fig. 15). Fluctuations of A_1 with periods of about ten days around a mean value might be related to the vacillations. Another evidence to discriminate between these phenomena is the importance of baroclinic process. That is, the variations between the single/double jet regimes are closely related to the variations of eddy heat flux around 50°S in the lower troposphere (Fig. 10).

It is well known that there exist 40–50 days oscillations of the zonal wind in the tropics (Madden and Julian, 1971). The period is about two months but the present phenomenon does not seem to have a close relation to the oscillations in the tropics, because the EOF of the first component shown in Figs. 4 and 14 has small modulus in the tropics.

In Section 4 we pointed out the relation between the time-averaged zonal wind and stationary planetary waves, which are defined as the time-averaged waves in the sub-periods. The amplitude of WN = 3 is large in the single jet regime, while WN = 2 is larger than WN = 3 in the double jet regime (Fig. 7). The predominance of WN = 3 in the single jet regime is reconfirmed by some observational studies on the planetary waves in the Southern Hemisphere. Hartmann (1977) showed that the amplitude of WN = 3 in July 1973 is largest in the middle-latitude troposphere and that the zonal wind has a single jet structure. Wallace and Hsu (1983) obtained a zonal wavenumber 3 pattern for the period July 6 – August 4 1981, which falls into the single jet regime as seen in Figs. 12, 13 and 15. However, we need more detailed analysis with longer data to show the relation between the WN = 3 pattern and the single jet regime because there also exists another type of WN = 3 pattern with an opposite phase 15°E–20°E (Mo, 1986).

It is interesting to refer some GCM experiments in relation to the variation of zonal mean wind in the Southern Hemisphere. Volmer *et al.* (1983) analyzed a 6-year integration of the ECMWF spectral model with forcings of a climatological annual cycle. They studied low-frequency variations of the results by making an EOF analysis of the 500 mb geopotential field after subtraction of the mean year. The first component of EOF has most of its variability in the Southern Hemisphere and has a strong zonal structure. Geostrophic winds expected from it are consistent with Fig. 14, in which the EOF has a node around 40°S. They also showed time-variation of the amplitude of this component. Strong anomalies lasting several weeks are observed; in the longest case the amplitude remained positive (corresponding to the double jet regime) during 86 days. The persistency is also the characteristics of our observational result (Fig. 15).

The double jet structure of the zonal mean wind is obtained in simple GCMs without land-sea contrast (Williams and Holloway, 1982; Hoskins, 1983). Although the multiplicity of planetary flow regimes was not their interest and not reported in their papers, it is worth while noting that the double jet structure is obtained for a similar lower boundary condition to the Southern Hemisphere without longitudinal contrast. As an observational fact the double jet structure of the zonal mean wind does not persist in the Northern Hemisphere where large longitudinal contrasts exist at the lower boundary.

7. Conclusion

The low-frequency variability of the zonal mean wind in the Southern Hemisphere troposphere observed in the present study is indicative of transitions between multiple planetary flow regimes. In the winter of 1983, in which the characteristics is very clear, there existed a single jet regime and a double jet regime. Both regimes have a characteristic duration of a month. In the single jet regime, the subtropical jet around 30°S and 200 mb exceeds 40 ms^{-1} and the stationary planetary waves of WN = 3 (and 4) have large amplitudes in addition to WN = 1. Some persistent diffluent patterns are observed in this regime around Australia and south-east of South America. In the double jet regime, on the other hand, the subtropical jet is weak and the polar night jet extends down to the surface at about 55°S. The dominant planetary waves are WN = 1 and 2.

In terms of the E–P flux diagnostics the difference of wave properties between the two regimes are summarized: The vertical component of the E–P flux $\overline{F(z)}$, which is proportional to the horizontal eddy heat flux, is larger in the single jet regime than in the double jet regime. Consequently, the wave driving $\overline{D_F}$, to which the vertical derivative of $\overline{F(z)}$ mainly contributes, has larger negative values in the single jet regime than in the double jet regime. The larger wave driving tends to keep the weaker westerlies around 60°S of the troposphere in the single jet regime.

The single/double jet regimes were observed also in the other three years 1980–1982. In these years there existed an intermediate state between the single and the double jet regimes. The time-variation among the regimes is irregular and there is no preferred period. Hence, the variation does not seem to result from an internal oscillation with an intrinsic frequency. The transition between the regimes is rather abrupt compared with the duration of each regime. Furthermore, the forced annual variation is not closely related with the variation among the regimes. These characteristics of the variations support the existence of multiple planetary flow regimes.

As our future observational study there remain some important questions: How are the single/double jet regimes sustained? When and how do the transitions take place? What triggers off the transition or what is a precursor?

Acknowledgments

We are grateful to J. R. Holton, T. Matsuno, T. Murakami, A. Sumi, and J. M. Wallace for their helpful discussions and valuable comments. Thanks are also due to A. Simmons for letting us know the numerical study by Volmer *et al.* This research was supported mainly by Grant-in-Aid for Scientific Research from the Ministry of Education and The Kurata Research Grant. SY's research was supported in part by JSPS Fellowship for Research Abroad (JSPS = Japan Society for the Promotion of Science). MS's research was supported in part by National Aeronautics and Space Administration through grants W15439 and W16215. The main body of the computations were performed at the Data Processing Center of Kyoto University with the use of the FACOM VP-100 and M-382 computers.

Appendix A

List of Symbols

φ	: latitude
p	: pressure
t	: time
z	: log-pressure height ($= -H \ln (p/p_s)$)
p_s	: reference pressure (1000 mb)
ρ_s	: reference density (density at $z = 0$)
ρ	: basic density profile ($=\rho_s \exp(-z/H)$)
f	: Coriolis parameter
N	: buoyancy frequency
H	: scale height
u	: zonal velocity
v	: meridional velocity
Φ_z	: vertical derivative of geopotential
$[(\ )]$	: zonal mean
$(\ )^*$	: departure from zonal mean
$(\ )$	: time average

References

Baldwin, M.P., H.J. Edmon, and J.R. Holton, 1985: A diagnostic study of eddy-mean flow interaction during FGGE SOP-1, *J. Atmos. Sci.*, **42**, 1838–1845.

Bengtsson, L., M. Kanamitsu, P. Kallberg and S. Uppala, 1982: FGGE research activities at ECMWF. *Bulletin*

A. M. S., **63**, 277–303.

Charney, J.G. and J.G. DeVore, 1979: Multiple flow equilibria in the atmosphere and blocking. *J. Atmos. Sci.*, **36**, 1205–1216.

Dole, R.M., 1982: *Persistent anomalies of the extratropical Northern Hemisphere wintertime circulation.* Ph.D. thesis, MIT, 226 pp.

Dunkerton, T., C.-P. Hsu and M.E. McIntyre, 1981: Some Eulerian and Lagrangian Diagnostics for a model stratospheric warming. *J. Atmos. Sci.*, **38**, 819–843.

Edmon, H.J., B.J. Hoskins and M.E. McIntyre, 1980: Eliassen-Palm cross sections for the troposphere. *J. Atmos. Sci.*, **37**, 2600–2616. (See also corrigendum, *J. Atmos. Sci.*, **38**, 1115, especially second last item.)

Geller, M.A., M.-F. Wu and M.E. Gelman, 1983: Troposphere-stratosphere (surface-55 km) monthly winter general circulation statistics for the Northern Hemisphere – four year averages. *J. Atmos. Sci.*, **40**, 1334–1352.

Hartmann, D.L., 1977: Stationary planetary waves in the Southern Hemisphere. *J. Geophys. Res.*, **82**, 4930–4934.

Hoskins, B.J., 1983: Modelling of the transient eddies and their feedback on the mean flow. *Large-scale dynamical processes in the atmosphere.* Eds, B.J. Hoskins and R.P. Pearce, Academic Press, 169–199.

Karoly, D.J., 1982: Eliassen-Palm cross sections for the Northern and Southern hemispheres. *J. Atmos. Sci.*, **39**, 178–182.

Legras, B. and M. Ghil, 1985: Persistent anomalies, blocking and variations in atmospheric predictability. *J. Atmos. Sci.*, **42**, 433–471.

Lorenz, E.N., 1968: Climatic determinism. *Meteor. Monogr.*, **8–30**, 1–3.

Madden, R.A. and P.R. Julian, 1971: Detection of a 40–50 day oscillation in the zonal wind in the tropical Pacific. *J. Atmos. Sci.*, **28**, 702–708.

Mechoso, C.R., D.L. Hartmann and J.D. Farrara, 1985: Climatology and interannual variability of wave, mean-flow interaction in the Southern Hemisphere. *J. Atmos. Sci.*, **42**, 2189–2206.

Mo, K.C., 1986: Quasi-stationary states in the Southern Hemisphere. *Mon. Wea. Rev.*, **114**, 808–823.

Mo, K.C. and M. Ghil, 1987: Statistics and dynamics of persistent anomalies. *J. Atmos. Sci.*, **44**, 877–901.

North, G.R., T.L. Bell, R.F. Cahalan and F.J. Moeng, 1982: Sampling errors in the estimation of empirical orthogonal functions. *Mon. Wea. Rev.*, **110**, 699–706.

Shiotani, M. and I. Hirota, 1985: Planetary wave-mean flow interaction in the stratosphere: A comparison between northern and southern hemispheres. *Quart. J. R. Met. Soc.*, **111**, 309–334.

Sutera, A., 1986: Probability density distribution of large-scale atmospheric flow. *Adv. in Geophys.*, **29**, 227–249.

Trenberth, K.E., 1979: Interannual variability of the 500 mb zonal mean flow in the Southern Hemisphere. *Mon. Wea. Rev.*, **107**, 1515–1524.

Trenberth, K.E., 1982: Seasonality in Southern Hemisphere eddy statistics at 500 mb. *J. Atmos. Sci.*, **39**, 2507–2520.

Trenberth, K.E., 1984: Interannual variability of the Southern Hemisphere circulation: Representativeness of the year of the Global Weather Experiment. *Mon. Wea. Rev.*, **112**, 108–123.

van Loon, H., 1972: Wind in the Southern Hemisphere, *Meteor. Monogr.*, **13–35**, 87–100.

Volmer, J.P., M. Deque and M. Jarraud, 1983: Large-scale fluctuations in a long-range integration of the ECMWF spectral model. *Tellus*, **35A**, 173–188.

Wallace, J.M. and D.S. Gutzler, 1981: Teleconnections in the geopotential height field during the Northern Hemisphere winter. *Mon. Wea. Rev.*, **109**, 784–812.

Wallace, J.M. and M.L. Blackmon, 1983: Observations of low-frequency atmospheric variability. *Large-scale dynamical processes in the atmosphere.* Eds, B.J. Hoskins and R.P. Pearce, Academic Press, 55–94.

Wallace, J.M. and H.H. Hsu, 1983: Ultra-long waves and two-dimensional Rossby waves. *J. Atmos. Sci.*, **40**, 2211–2219.

Webster, P.J. and J.L. Keller, 1975: Atmospheric variations: Vacillations and index cycles. *J. Atmos. Sci.*, **32**, 1283–1300.

Williams, G.P. and J.L. Holloway Jr., 1982: The range and unity of planetary circulations. *Nature*, **297**, 295–299.

南半球で解析された惑星規模の循環形態の多様性

余田成男・塩谷雅人・廣田　勇
（京都大学理学部地球物理学教室）

南半球対流圏における大気大循環の長期変動（季節内変動）を調べた。用いた資料はアメリカ気象局（NMC）で毎日解析されている全球ジオポテンシャル高度場である。

1983年冬季には，帯状平均した地衡風は2つの典型的な子午面分布をしていた。それぞれの特徴より，単一ジェット型，二重ジェット型と呼ぶことにする。両者ともに約1ヵ月の持続期間を持ち，交互に2回ずつ出現した。単一ジェット型の折には，亜熱帯ジェットが強く，波数3型の循環である。他方，二重ジェット型の折には，亜熱帯ジェットが弱く，成層圏極夜ジェットが南緯55° 辺で地表面までその裾野を広げている。500 mb 高度場の時間平均図をみると波数2型である。これらの循環形態は1980～1982年の冬季にも見出される。

単一ジェット型と二重ジェット型の平均帯状風にともなう波の活動性の違いについて，準地衡風E-Pフラックスとその収束・発散を用いて調べた。E-Pフラックスの鉛直成分（水平方向のうず熱輸送に比例）は中緯度対流圏で二重ジェット時より単一ジェット時のほうが大きい。その結果，E-Pフラックスの収束は，中高緯度対流圏界面付近で，二重ジェット時より単一ジェット時のほうが大きい。つまり，より大きなE-P フラックスの収束は50～60° S の対流圏において，より弱い西風（すなわち単一ジェットの構造）を維持する傾向にある。

経験的直交関数展開法（主成分解析）を用いて，帯状平均東西風の2次元（子午面内）変動を特徴づける帯状示数を定義した。40%以上の寄与率をもつ第1主成分の振幅がその示数で，単一ジェット型と二重ジェット型の間の変動をうまく捉えることができる。この帯状示数の変動は，固有の周期を持つような内部振動ではない。ある循環形態から別の形態への移り変りは，それぞれの形態の持続期間に比べて短かい。また，この変動は地球公転によって生じる強制振動（年変動）との明白な関連はない。これらの事実は「南半球で見い出された惑星規模循環の季節内変動を，同一外部条件の下での複数の循環形態間の遷移として択えることができる。」という解釈を支持する。